EARTH SURFACE PROCESSES AND LANDFORMS
Earth Surf. Process. Landforms **39**, 928–942 (2014)

Published online 2 December 2013 in Wiley Online Library
(wileyonlinelibrary.com) DOI: 10.1002/esp.3499

Bedload transport measurements with impact plate geophones: comparison of sensor calibration in different gravel-bed streams

Dieter Rickenmann,[1]* Jens M. Turowski,[1,2] Bruno Fritschi,[1] Carlos Wyss,[1] Jonathan Laronne,[3] Ronel Barzilai,[3] Ian Reid,[4] Andrea Kreisler,[5] Johann Aigner,[5] Hugo Seitz[5] and Helmut Habersack[5]

[1] Swiss Federal Research Institute (WSL), Mountain Hydrology and Mass Movements, Birmensdorf, Switzerland
[2] Helmholtz Centre Potsdam, GFZ German Research Centre for Geosciences, Potsdam, Germany
[3] Geography and Environmental Development, Ben-Gurion University of the Negev, Beer Sheva, Israel
[4] Department of Geography, Loughborough University, Leicestershire, UK
[5] Institute of Water Management, Hydrology and Hydraulic Engineering, University of Natural Resources and Life Sciences, Vienna, Austria

Received 1 July 2013; Revised 21 October 2013; Accepted 29 October 2013

*Correspondence to: Dieter Rickenmann, Swiss Federal Research Institute (WSL), Mountain Hydrology and Mass Movements, Birmensdorf, Switzerland.
E-mail: dieter.rickenmann@wsl.ch

ESPL
Earth Surface Processes and Landforms

ABSTRACT: Indirect bedload transport measurements have been made with the Swiss plate geophone system in five gravel-bed mountain streams. These geophone sensors record the motion of bedload particles transported over a steel plate mounted flush with the channel bed. To calibrate the geophone system, direct bedload transport measurements were undertaken simultaneously. At the Erlenbach in Switzerland, a moving-basket sampler was used. At the Fischbach and Ruetz streams in Austria, a Helley–Smith type bedload sampler provided the calibration measurements. A Bunte-type bedload trap was used at the Rofenache stream in Austria. At the Nahal Eshtemoa in Israel, Reid-type slot bedload samplers were used. To characterize the response of the geophone signal to bedload particles impacting on the plate, geophone summary values were calculated from the raw signal and stored at one second intervals. The number of impulses, i.e. the number of peaks above a pre-defined threshold value of the geophone output signal, correlated well with field measured gravel transport loads and was found to be a robust parameter. The relations of impulses to gravel transport loads were generally near-linear, but the steepness of the calibration relations differed from site to site. By comparing the calibration measurements from the different field sites and utilizing insights gained during preliminary flume experiments, it has been possible to identify the main factors that are responsible for site specific differences in the calibration coefficient. The analysis of these calibration measurements indicates that the geophone signal also contains some information about the grain size distribution of bedload. Copyright © 2013 John Wiley & Sons, Ltd.

KEYWORDS: bedload transport; geophone sensor; indirect measurement; calibration; gravel-bed stream; Swiss plate geophone

Introduction

Indirect methods of measuring bedload transport in mountain streams can provide useful high-resolution data for fluvial sediment transport studies. Indirect techniques include geophones placed in or near the streambed (e.g. Thorne, 1986a, 1986b; Taniguchi *et al.*, 1992; Thorne and Hanes, 2002; Downing *et al.*, 2003; Froehlich, 2003, 2010; Mizuyama *et al.*, 2010a, 2010b; Rickenmann *et al.*, 2012), hydrophones and vibration sensors (Bänziger and Burch, 1990; Bogen and Møen, 2003; Richardson *et al.*, 2003; Rickenmann and McArdell, 2007, 2008; Krein *et al.*, 2008; Møen *et al.*, 2010), and underwater microphones (Barton *et al.*, 2010; Belleudy *et al.*, 2010; Camenen *et al.*, 2012). Non-invasive techniques have the advantage of minimizing local and temporal changes in the flow field near the sensor. Some important conclusions from the International Bedload Surrogate Monitoring Workshop, held in April 2007 in Minneapolis, USA (Gray *et al.*, 2010), are: (i) indirect bedload measuring methods have the advantage of providing continuous records of bedload transport activity both in time and over a cross-section; (ii) controlled laboratory experiments are important for a better understanding of the factors influencing the calibration of these measuring methods; and (iii) additional field calibration of the sensors is necessary to obtain a reasonable measuring accuracy.

Hydrophones (underwater microphones) are placed in a river environment with a supporting structure (e.g. close to one bank) and sense acoustic waves or the underwater sound generated by inter-particle collisions during bedload movement are recorded (Barton *et al.*, 2010). Recently, hydrophones have been tested in an Alpine mountain river and compared with impact plate geophone measurements (Geay, 2013). Hydrophones can detect bedload transport activity integrated over a certain area of the channel, but they are also sensitive to any other noise present in the river, e.g. that generated by turbulence (hydrodynamic noise) or vessel traffic (Bassett

et al., 2013). Impact pipes (also called Japanese pipe hydrophones) measure the sound within an air-filled steel pipe that is generated by impacting bedload particles and they are typically partly embedded in the streambed and aligned transversally to the stream flow (Mizuyama *et al.*, 2010a, 2010b). Impact columns represent another indirect method which has been applied in gravel-bed streams. An example of an impact column is the gravel-transport sensor (GTS) developed by Downing (2010), which is installed vertically on the streambed. When a particle strikes the column, an electric charge is generated, the magnitude of which depends on the force of impact and the momentum of the particle. The design of this system has been optimized through laboratory testing (Papanicolaou and Knapp, 2010). Another type of impact sensor consists of an accelerometer attached to a metal plate (15 cm × 13 cm × 0.6 cm in size) that lies flush with the channel bed, and it has been used to assess bedload transport activity in a gravel-bed stream in the UK (Reid *et al.*, 2007; Raven *et al.*, 2010).

In this paper the focus is on impact plate geophone measurements of bedload transport. The Erlenbach is a hydrologic research catchment of the Swiss Federal Research Institute (WSL). Bedload transport observations here have been available since 1982 from regular surveys of sediment retention basins and, since 1986, from a piezoelectric bedload impact sensors (PBISs), which were replaced by geophone sensors in 1999. PBISs and geophone sensors are indirect methods of estimating the volume of bedload transport of coarse sediment and have provided continuous measurements of transport intensities for more than 25 years in the Erlenbach (Rickenmann, 1997; Rickenmann and McArdell, 2007; Turowski *et al.*, 2009; Rickenmann and Fritschi, 2010; Rickenmann *et al.*, 2012). During the last 15 years, a geophone measuring system using bed-parallel steel plates of standard dimensions (referred to hereafter as the Swiss plate geophone) has been installed at several gravel-bed streams (Turowski and Rickenmann, 2011; Turowski *et al.*, 2011; Rickenmann *et al.*, 2012). At many of these sites, direct bedload measurements are available to calibrate the geophone measurements. The objectives of this paper are: (i) to present and compare calibrations for five streams; (ii) to present and discuss several integrated (pre-processed) parameters that characterize the geophone signal, which can be used to develop calibration relations for bedload mass; (iii) to discuss the influence of grain size and of mean flow velocity on the geophone signal; and (iv) to identify site-independent and site-specific elements characterizing the signal response of the geophone measuring system. Finally, the possibility of using a flume-based calibration relation for a given site is briefly discussed.

Field Sites and Calibration Measurements

Overview of field sites and geophone measurements

The first indirect bedload transport measurements using impact plates occurred in the Erlenbach in 1986 with the aim of continuously monitoring the intensity of bedload transport and its relation to stream discharge (Bänziger and Burch, 1990; Rickenmann, 1997; Hegg *et al.*, 2006). An array of steel plates is typically installed flush with the surface of a sill or check dam, a location where there is only a small probability that bedload grains will be deposited during a flood event. The original PBIS system using a piezoelectric crystal had been tested and calibrated mainly at two field sites, the Erlenbach and the Pitzbach (Rickenmann and McArdell, 2007, 2008), but also in flume experiments using sediment particles from the Erlenbach (Etter, 1996). A further check on the relative variability of the PBIS signal was achieved by installing in the Erlenbach two PBIS arrays, 14 m apart (Rickenmann and Fritschi, 2010). Some of these PBISs reached the end of their life towards 1999. To standardize instrumentation, the piezoelectric crystals were replaced with geophones at the end of 1999, reducing the number of active sensors to six (Rickenmann *et al.*, 2012).

During the last 15 years, the geophone measuring system using bed-parallel steel plates of standard dimensions has been employed in many streams, primarily in Switzerland and Austria (Table I). The Vogelbach is in the Alptal and is another hydrological observatory operated by WSL in the vicinity of the Erlenbach. Other field sites are maintained by hydropower companies in collaboration with WSL (Fischbach, Ruetz, Ötztaler Aache, Pitzbach, Riedbach, Schweibbach), or operated

Table I. Overview of field sites with impact plate geophone sensor (GS) measurements for bedload transport estimation.

Stream	Location	Drainage area (km^2)	Operation (sensor type)	Calibration
Erlenbach (retention basin)	Alptal, Schwyz, CH	0.7	1986–1999 (PBIS) 2000+ (GS)	yes
Erlenbach (bridge)	Alptal, Schwyz, CH	0.5	1995–1997 (PBIS), 2002+ (GS)	
Vogelbach	Alptal, Schwyz, CH	1.6	1999+ (GS)	
Pitzbach	Pitztal, Tyrol, A	27	1994–1995 (PBIS)	yes
Spissibach	Leissigen, Berne, CH	2.5	1998–2010 (PBIS)	yes
Rofenache	Vent, Tyrol, A	98	2000+ (GS)	yes
Drau[a]	Lienz, Tyrol, A	1876	2002+ (GS)	
Drau[a]	Dellach, Carynthia, A	2300	2006+ (GS)	yes
Isel[a]	Lienz, Tyrol, A	1199	2006+ (GS)	
Schweibbach	Eisten, Valais, CH	9.7	2007+ (GS)	
Fischbach	Mühlau, Tyrol, A	71	2008+ (GS)	yes
Ruetz	Mutterbergalm, Tyrol, A	28	2008+ (GS)	yes
Riedbach	Grächen, Valais, CH	18.7	2009+ (GS)	yes
Nahal Eshtemoa	Negev Desert, Israel	119	2009+ (GS)	yes
Navisence	Zinal, Valais, CH	82	2011+ (GS)	yes
Ötztaler Aache	Sölden, A	197	2011+ (GS)	yes
Urslau[a]	Maria Alm, Salzburg, A	55	2011+ (GS)	yes
Elwha River	Washington, USA	833	2009+ (GS)[b]	yes

Note: Some of the earlier measurements were made with piezoelectric bedload impact sensors (PBISs). "+"indicates start year of monitoring. (CH = Switzerland; A = Austria).

[a]These comparable impact plate geophone systems are part of integrated bedload monitoring stations (Habersack *et al.*, 2010).

[b]In the Elwha River, acceleration sensors are also installed.

independently by other research institutes and agencies (Navisence, Rofenache, Drau, Isel, Urslau, Nahal Eshtemoa, Elwha River). The channels represent a wide range of conditions, from small step-pool streams (Erlenbach, Vogelbach), glacier-fed gravel-bed streams (Fischbach, Ruetz, Pitzbach, Rofenache, Riedbach, Schweibbach, Navisence) and larger mountain rivers (Drau, Isel, Elwha River) to an ephemeral desert stream where events are discrete, flash floods (Nahal Eshtemoa). For more than half of these streams, independent, direct measurements of bedload transport are available for the calibration of the indirect method (Table I). Comparable impact plate geophone systems on the Drau, Isel and Urslau stream are part of integrated bedload monitoring stations (Habersack *et al.*, 2010).

In this study, we present the calibration measurement obtained in Erlenbach, Fischbach, Ruetz, Rofenache, and Eshtemoa (Figure 1). At all of these sites, the geophone signal is sampled at a rate of 10 kHz. During normal flow monitoring conditions (i.e. when there are no calibration measurements), a pre-processing of the geophone signal provides summary values; due to data storage limitations, the raw signal is not recorded. During calibration of the geophone system, raw signals have been recorded while direct bedload transport measurements were being made. This has yielded between 17 and 46 pairs of records per site, except in the Eshtemoa, where infrequent bedload events mean that only four data pairs have been obtained so far. The sampling periods ranged from three seconds to one hour, depending on contemporaneous bedload transport rate. The field sites and the calibration measurements are described in more detail later (see also Table II).

The geophone sensors are fixed in a cylindrical aluminum case mounted on the underside and in the middle of a 0.36 m long, 0.50 m wide, and 0.015 m thick steel plate. The sensors are acoustically isolated from the frame and other plates using elastomer elements. During bedload transport, gravel particles slide, roll or saltate over the steel plate, which is installed flush with the streambed. The plate transmits to the inertial mass moving in a coil of the geophone sensor the impact shocks and, thereby, an electrical potential is produced. The standard geophone sensor uses a magnet in a coil as an inductive element. The magnet moves with the steel plate and induces a current in the coil which is proportional to the velocity of the magnet. Whenever the voltage exceeds a preselected threshold amplitude value, A_{min}, the shock is recorded as an impulse.

Based both on laboratory experiments using sediment from the Erlenbach (Etter, 1996) and on field tests during comparatively low flows, the critical grain size registering an impulse with the PBIS was estimated to be between 14 and 38 g, corresponding to a mean diameter of 10 to 30 mm for a sphere of quartz (Rickenmann and McArdell, 2007). Flume experiments using sediment from the Erlenbach were conducted with a flow velocity of 2.3 m/s, corresponding approximately to the flow velocity at a discharge of 0.4 m^3/s in the Erlenbach and representing flow conditions near the beginning of bedload transport. These flume tests indicated that the number of impulses per unit mass strongly increases for uniform-sized particles with mean weights increasing progressively from 25 to 50 g and then to 75 g, corresponding with mean *b*-axes of 26, 31, and 37 mm (Böckli, 2011). This revealed that the threshold particle size or weight appears to be somewhat larger in the case of the geophone than was the case for the PBIS it replaced.

Signal pre-processing and geophone summary values

Typically following impact of a single particle on the steel plate, oscillation of the geophone signal is attenuated over an interval of about 5–20 ms, as illustrated by dropping a particle

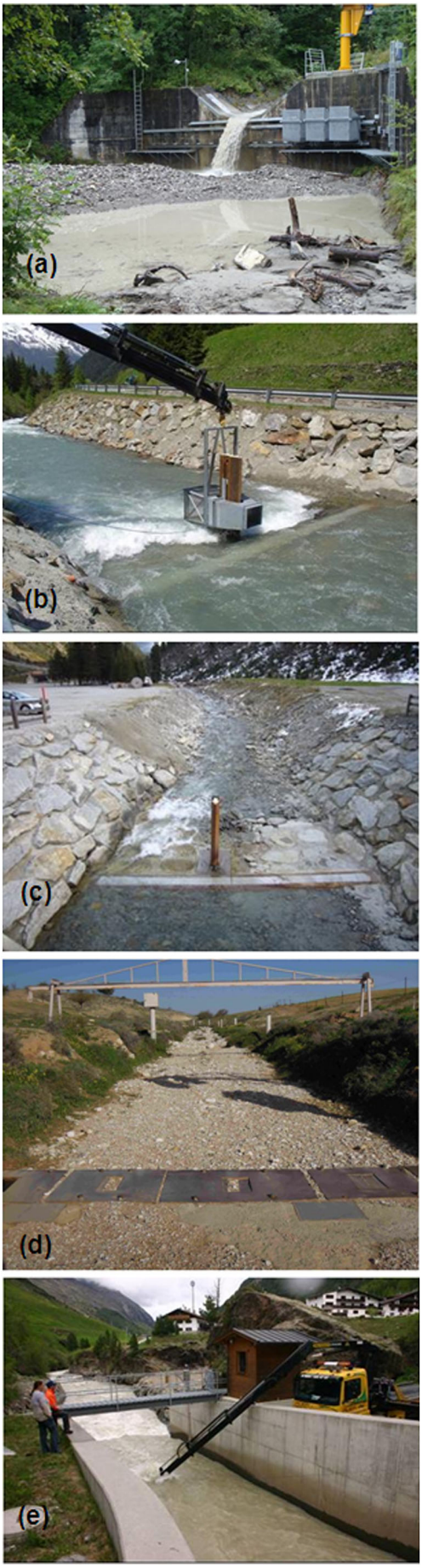

Figure 1. Field sites having geophone calibration measurements: (a) Erlenbach, (b) Fischbach, (c) Ruetz, (d) Nahal Eshtemoa, (e) Rofenache. This figure is available in colour online at wileyonlinelibrary.com/journal/espl

Table II. Catchment and channel characteristics at the field sites and range of typical parameters for the conditions during the geophone calibration measurements.

	Erlenbach	Fischbach	Ruetz	Rofenache	Eshtemoa
Catchment parameters					
Drainage area (km^2)	0.7	71	28	98.1	112
Maximum elevation (m)	1655	3497	3474	3738	870
Site elevation (m)	1110	1540	1684	1891	410
Mean annual precipitation (mm)	2300			1541	220–235
% glacier	0	17	22	28	0
Channel parameters (measuring site)					
Gradient upstream of geophone site S (%)	16/10[a]	2.0	5.5	3.8	0.75
Stream bed width (m)	3	8.5	8.5	6.5	6
Bed surface D_{84} (m)	0.29	0.14	0.33	—	0.038
Bed surface D_{50} (m)	0.07	0.04	0.06	—	0.017
Parameter range for calibration periods					
Period of calibration measurements used in this study	2009– 2012	2008–2011	2008–2011	2009– 2010	27 March 2010
No. of calibration measurements used in this study	46	28	17	43	4
Maximum unit discharge q_{max} (m^2/s)	0.455	1.91	0.97	7.2	1.99
Minimum unit discharge q_{min} (m^2/s)	0.087	0.54	0.41	3.4	0.36
Maximum mean flow velocity V_{max} (m/s)	3.54	2.79	1.88	6.19	2.80
Minimum mean flow velocity V_{min} (m/s)	2.53	1.51	1.02	4.94	1.80
Maximum unit bedload transport rate, $q_{b,max}$ (kg/s m)	3.96	7.20	0.214	36.5	4.00
Minimum unit bedload transport rate, $q_{b,min}$ (kg/s m)	0.015	0.0050	0.0063	0.5	0.069
Bedload samples: maximum D_{max} (m)	0.200	0.350	0.150	0.26	0.128
Bedload samples: minimum D_{max} (m)	0.042	0.030	0.050	0.10	0.090
Bedload samples: mean P_i (%) for $D > 20$ mm	54	71	63	72	59/57[b]
Bedload samples: mean P_i (%) for $D > 30$ mm	33	53	43	59	37/32[b]
Bedload samples: mean P_i (%) for $D > 40$ mm	22	44	33	50	22/19[b]
Bedload samples: maximum weight ($D > 10$ mm) (kg)	348	431	128	90.1	147
Bedload samples: mean weight ($D > 10$ mm) (kg)	130	67.0	23.4	33.0	80.3
Sampling frequency of geophone signal (for calibration measurements) (kHz)	10	10	10	10	10
Recording interval of geophone summary values during calibration measurements (s)	1	1	1	—	1
Sampling duration of calibration measurements (s)	44–608	30–3600	600–3600	3–15	194–1619
Recording interval of geophone summary values during normal flow monitoring (s)	60	900	900	60	1
Threshold for *IMP* counts (A_{min}) (V)	0.1	0.07[c]	0.07[c]	0.1	0.1

Note: P_i are percentage weight of grains coarser than a given size D_i (where i is grain size in milimetres). The P_i values given in Table II are average values for all samples and refer to bedload with $D > 10$ mm. The q_b values also refer to bedload with $D > 10$ mm.
[a]Erlenbach: first value of S refers to artificial approach channel, second value to natural stream reach upstream of approach channel.
[b]Eshtemoa: First value of P_i refers to left centre sampler during calibration event, second value is average value according to Powell *et al.* (2001, figure 1).
[c]Geophone signal is dampened by about 30%.

onto the steel plate (figure 3 of Rickenmann *et al.*, 2012). Even a single particle impact may result in multiple impulse counts, as depicted in Figure 2. Prior to recording the raw signal at some of the field sites, we had decided to store several signal summary values that were thought prospectively useful for the development of calibration relations. The definitions of these geophone signal summary values are given in Table III and illustrated in Figure 2.

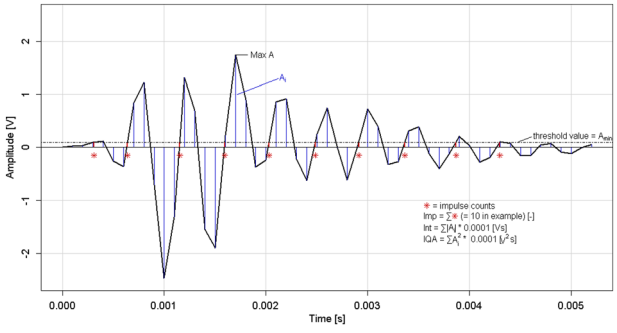

Figure 2. Definitions of recorded geophone values characterizing the signal over a given recording interval (which is one second during calibration). The time constant 0.0001 seconds is valid for a sampling rate of 10 kHz. This figure is available in colour online at wileyonlinelibrary.com/journal/espl

Firstly, *Sum IMP* (summed impulse counts) values were found to correlate reasonably well with bedload mass or volume transported (Rickenmann and McArdell, 2007, 2008; Rickenmann and Fritschi, 2010; Rickenmann *et al.*, 2012). Secondly, flume experiments had indicated that the amplitude of the signal (*MaxMaxA*, *Sum Max*) and the number of impulses depend on the size of particles transported over the plates (Etter, 1996; Turowski and Rickenmann, 2009; Böckli, 2011; Hegglin, 2011; Morach, 2011). Thirdly, the integral of the geophone signal (*Sum INT*) might be expected to provide a combined measure related to both the number of impulses (frequency information) and the strength of the signal (amplitude information). Fourthly, since the geophone signal is proportional to the velocity of the deformation of the steel plate, the momentum transmitted by the particles onto the plate should be related to the acoustic energy of the signal which is proportional to the value obtained by summing the squared amplitudes values (*Sum IQA*).

Table III. Definition of recorded geophone summary values characterizing the signal over a given recording interval, which is one second for the calibration measurements.

IMP (−)	*Impulses*: Each crossing of positive amplitude values during the rising limb over the threshold amplitude value A_{min} (0.1 V or 0.07 V; see Table II) is counted as impulse; summed impulse values are recorded each second.
Sum IMP (−)	*Sum Impulses*: Sum of IMP values (of each second) over the calibration recording period.
MaxA (V)	*Maximum Amplitude*: Maximum amplitude value per second; one value is recorded each second (only positive range of amplitudes is considered).
Sum Max (V)	*Sum Maxima Amplitude*: Sum of *MaxA* values (one value per second interval) over the calibration recording period.
Sum Max_IP (V)	*Sum Maxima Amplitude*: Sum of *MaxA* values over the calibration recording period, only for those one second intervals for which $IMP > 0$. *Sum Max_IP* includes less "noise" than *Sum Max* because at least one amplitude value $> A_{min}$ occurred in a one second interval.
MaxMaxA (V)	*Maximum of Maximum Amplitudes*: Largest maximum amplitude value observed during recording interval.
INT (V s)	*Integral*: Sum of absolute amplitude values multiplied by 0.0001 s (at the 10 kHz measuring rate); one value is recorded each second.[a]
Sum INT (V s)	*Sum of INT*: *INT* values (of each second) summed over the calibration recording period.[a]
Sum INT_IP (V s)	*Sum of INT of Impulse-period*: *INT* values summed over the calibration recording period only for those second intervals with $IMP > 0$. *Sum INT_IP* includes less "noise" than *Sum INT* because at least one amplitude value $> A_{min}$ occurred in a one second interval.[a]
Sum INT_IP_noN (V s)	*Sum of INT of Impulse-period without noise*: *Sum INT_IP* values are corrected by subtracting the average noise over the integration period.[a]
IQA (V^2 s)	*Quadratic Integral*: Sum of squared amplitude values multiplied by 0.0001 s (at the 10 kHz measuring rate); one value is recorded each second.[b]
Sum IQA (V^2 s)	*Sum of IQA*: *IQA* values (of each second) summed over the calibration recording period.[b]
Sum IQA_IP (V^2 s)	*Sum of IQA of Impulse-period*: *IQA* values summed over the calibration recording period only for those second intervals with $IMP > 0$. *Sum IQA_IP* includes less "noise" than *Sum IQA* because at least one amplitude value $> A_{min}$ occurred in a one second interval.[b]

[a]For Fischbach and Ruetz only available for years 2008–2009.
[b]For Fischbach and Ruetz only available from 2010 onwards.

These four basic summary values – *IMP*, *MaxA*, *INT*, and *IQA* – are used to derive the other summary values listed in Table III. If the basic summary values are integrated over some observation time (*Sum Max*, *Sum INT*, *Sum IQA*), they will include some "noise" for periods with no significant bedload transport, i.e. for time periods with amplitude values $< A_{min}$. Therefore, we have also determined summary values that include less "noise" by summing only those one second intervals during which at least one amplitude value $> A_{min}$ occurred (*Sum Max_IP*, *Sum INT_IP*, *Sum IQA_IP*); the notation *_IP* refers to one second intervals for which at least one impulse was recorded (impulse period).

Erlenbach field site and calibration measurements

At the Erlenbach field site, there is a stream gauging station some 50 m upstream of the sediment retention basin. An array of Swiss plate geophones was embedded in the large check dam at the entrance to the retention basin (Figure 1a). Six geophone sensors replaced the old piezoelectric sensors in 2000 and were installed in the lowest part of the cross-section. The geophone (and the previous PBIS) measurements were first calibrated by comparison with sediment volumes determined by regular surveys of the deposits in the retention basin. From 2009, a moving basket sampler was used to obtain further calibration measurements of the geophone system (Rickenmann *et al.*, 2012). Depending on water discharge and bedload transport activity, a metal basket mounted on rails is moved automatically into the flow discharging from a large check dam. The metal basket is 1 m wide (laterally), 1 m long (in the flow direction) and 1 m high, with an additional wedge-shaped metal grid of maximum 0.5 m height (at the downstream end) to prevent ejection or bypassing of bedload particles near the front of the basket at higher flows. The walls and floor of the basket are made of 10 mm wire mesh, to collect all grain sizes which potentially produce geophone impulses. During calibration measurements, the basket is stopped in the middle of the check dam, so that the two lowest geophone plates are in line with the opening of the basket; this guarantees a complete sampling of all bedload particles that have travelled over the two middle geophone plates.

Geophone calibration measurements were obtained with the moving basket system during 2009–2012. From a total of 61 measurements, 46 were selected (Table II). Similar to the analysis presented by Rickenmann *et al.* (2012), measurements when mean discharge $Q < 0.3\ m^3/s$, or mean unit bedload transport rate (for $D > 10$ mm) $q_b < 0.005$ kg/s m, or sampling duration $T < 20$ s were excluded. The first two criteria refer to conditions with very low bedload flux and only a small proportion of mobile grains with $D > 20$ mm – an approximate lower detection limit for the geophone system. The criterion involving minimum sampling time limits uncertainty associated with the time for the basket to move completely into (or out of) the measuring cross-section, which is seven to eight seconds. Based on measured discharge Q at the nearby gauging station, and occasional on-site measurements of the flow cross-section and surface velocity, an empirical equation has been developed to estimate mean flow velocity V_w at the geophone measuring site: $V_w = 3.3\ Q^{0.25}$. (Mean flow velocity is used later to explain site-specific differences in the calibration relation.)

Fischbach and Ruetz field sites and calibration measurements

The Fischbach and Ruetz field sites are operated by the Tyrolean Water Power Company (TIWAG). They are located in partly glaciated catchments in the Tyrolean Alps. At both field sites, water discharge and bedload transport have been monitored since 2008. The stream cross-section is trapezoidal at each measuring site, with the banks protected by riprap and inclined at 45°. The geophone sensors are installed in an 8.7 m wide sill installed across the stream bed (Figures 1b and 1c). The sill is protected with riprap on the upstream and downstream side, and it is laterally inclined at 5%, which improves the discharge measurements at low flows. At the top of each sill, there is an

array of 16 steel plates of standard dimensions. Every second steel plate is equipped with a geophone sensor, so that there are a total of eight sensors at each site.

For the calibration measurements, a streamlined metal pillar was installed 50 cm downstream of geophone plate no. 8. The metal pillar has a height of 2.5 m and a maximum width of 25 cm and ensures that a pressure-difference type metal basket sampler fits snugly onto the bed and can be held in place during the bedload sampling operation (Figure 1b). The aperture of the basket is 50 cm by 50 cm, the same width as geophone plate no. 8. The basket has a notch (cut-out) at a downstream distance of 45 cm from the aperture. The notch is somewhat larger than the cross-section of the metal pillar, and the inside of the notch is equipped with rollers. This system allows an exact positioning of the basket during geophone calibration measurements. The maximum width of the basket is 90 cm and the total length is 210 cm. During operation the upper surface of the sampler is horizontal while the lower surface is declined at 15% in the downstream direction, in line with the artificial bed in the vicinity of the metal pillar. Over the 80 cm tail-end of the sampler, the top and sidewall surfaces of the basket are made of 10 mm metal wire mesh. The total volume of the basket is about 0.91 m^3.

The calibration measurements used here were obtained by TIWAG in both streams during the summer months of 2008 to 2011. A total of 28 measurements from the Fischbach and 17 measurements from the Ruetz have been used in this analysis (Table II). The maximum sample mass caught in the sampler was 518 kg in the Fischbach; assuming a bulk density of 1600 kg/m^3, the bedload volume of this sample was about 0.32 m^3 or about a third of the total sampler volume. Two calibration measurements from the Fischbach could not be used due to overfilling of the sampler. The grain size distribution of the samples was determined by sieve analysis. A line-by-number analysis was performed in both streams in October 2009 to estimate the grain size distribution of the bed surface upstream of the geophone sites. Stage-discharge relations were determined by TIWAG based on flow velocity measurements made at the two sites. To estimate mean flow velocity at the geophone sites, the variable power equation of Ferguson (2007), with coefficients as proposed by Rickenmann and Recking (2011), was used. These estimates were within −20% (Fischbach) and ±20% (Ruetz) of the mean flow velocity determined from each stage–discharge relation.

In contrast with the other sites, the threshold amplitude value A_{min} used to determine *IMP* values was set at 0.07 V at the Fischbach and Ruetz (Tables II and III). The reason is that the first regular geophone recordings in the Fischbach had shown maximum amplitudes in excess of 10 V, the upper limit of the recording system. To increase the resolution of large amplitudes, the raw signal was dampened by about 30%. To compensate for lower signal strength in relation to the impulse counts, the threshold amplitude value A_{min} was also reduced by 30% when compared with a typical value of 0.1 V used at all other sites.

Rofenache field site and calibration measurements

The gauging station Rofenache Vent is operated by the Tyrolean Hydrographic Service. Bedload transport measurements have been conducted since 2008 by the University of Natural Resources and Life Sciences, Vienna. The measuring station is located in the Tyrolean Alps, 1891 m above sea level. The glacial melt-water regime is characterized by low flow in winter and peak flows in July and August (Mader *et al.*, 1996) because a large part of the catchment is covered with glacier (Müller *et al.*, 2009). Diurnal fluctuations of discharge, varying with air temperature, are typical at this gauging station. The mean annual discharge at the measuring station is 4.5 m^3/s. The gauging station is set in a rectangular concrete flume 6.5 m wide (Figure 1e). A Swiss plate geophone system is installed, consisting of an array of 12 geophone plates set flush with the bed of the concrete flume.

Calibration measurements were made with a basket sampler, a development and adaptation of a bedload trap developed by Bunte and Abt (2003) and consisting of a steel-frame, a sampler bag and steel bar. The intake is 0.44 m wide and 0.26 m high with a mesh size of 3.5 mm × 6.5 mm, which means that 6.5 mm is the smallest particle size that can be sampled. The steel bar is mounted centrally on the upper part of the intake frame, using a uniaxial rotary joint. This rotatable connection enables the sampler intake to turn to face the mean flow direction in response to the fluvial forces. The basket sampler can be mounted on a mobile crane at the upper end of the steel bar. Two tensioning ropes, fixed on either side of the steel frame and to both riverbanks, prohibit the sampler from drifting downstream and keep the sampler in the stream centre. Due to restricted accessibility, direct bedload measurements had to be made about 4–5 m upstream of the geophone plates; they were made in the middle of the flume profile. Taking bedload samples upstream of the geophones causes the dilemma that there is no direct match between geophone impulses and calibration samples.

Geophone recordings are available at one minute intervals, the summary values thus representing integrated values over 60 seconds duration. The mean readings of two geophone plates placed in the middle of the cross-section were compared with the direct bedload measurements. As the bedload samples were collected upstream of the geophone plates, it was decided to use only measurements with a maximum sampling duration of 15 seconds. Assuming steady (over 60 seconds) and laterally uniform (over 1 m central width) bedload transport, this limits the potential error to an underestimation of about 13% of the true value of geophone impulses. In the period from 2008 to 2011, 43 basket sampler measurements were undertaken with 15 seconds maximum sampling duration. Specific bedload transport varied between 0.5 and 36.5 kg/s m. For our analysis, bedload material larger than 10 mm was considered. Mean flow velocity was determined from a relation between measured discharge and water depth.

Nahal Eshtemoa field site and calibration measurements

Nahal Eshtemoa is one of several sub-parallel river channels that drain the semi-arid, south-western flank of the Judean Mountains. These channels merge with others of the Beer Sheva Depression to form the Nahal Besor, which debouches to the eastern Mediterranean through Gaza (Alexandrov *et al.*, 2009). The Eshtemoa has an ephemeral flow regime and the channel is devoid of water for > 99% of time. Floods are flashy, responding variously but abruptly to either low-intensity frontal or high-intensity convectional rain storms (Alexandrov *et al.*, 2007). The average time-of-rise of the flood hydrograph at the monitoring station is 16 minutes (Reid *et al.*, 1998). The channel bed at the monitoring station is 6 m wide, it has near-vertical banks of 1.2 m and a longitudinal slope (mirrored by the flood-water surface) of 0.0075. It is typified by an alternating longitudinal pattern of bars and flats, the bars having a roughness determined by a mixture of cobbles, pebbles and occasional boulders, whilst the flats consist of pebbles and

granules and occasional cobbles (Powell *et al.*, 2012). Although both of these bedform types contribute material to bedload, the majority is derived from the flats and comprises pebbles, granules and sand. Coarser grains, including cobbles and boulders, are mobilized at higher boundary shear stresses and the size-range of the bed material is proportionally represented in the bedload at transport stages ≥ 4.5 $\tau/\tau c$ (Powell *et al.*, 2001; Cohen *et al.*, 2010). This wide range of mobile particle sizes is of particular significance when considering the performance of geophones in this stream environment.

Bedload is monitored continuously in the longitudinal middle of a straight reach of the channel by five independent, fully-automatic, Reid-type (also called Birkbeck-type) horizontal-slot pit-samplers set across the channel width (Bergman *et al.*, 2007). Sampler slot width has been set to 110 mm for three of the samplers; at the other two samplers it is 165 mm. The samplers were supplemented in autumn 2009 by two Swiss plate geophones that are set flush with the bed surface and located immediately downstream of, and between, the Left-Centre (LC) and Centre and the Right-Centre (RC) and Right (R) slot pit-samplers (Figure 1d). Typically, bedload transport is quite uniform over the cross-section, with some reduction observed for the samplers closest to the banks (Powell *et al.*, 1998, 1999).

During the flood event of 27 March 2010, four sampling durations in the range 4–32 minutes could be used for geophone calibration. The LC sampler (with a slot width of 110 mm) gave plausible measurements (and a similar weight increase as sampler RC). These measurements were averaged over 30 second intervals. The geophone signal at the Eshtemoa generally shows a much weaker response than at other sites. Therefore, we used a mean of values recorded by the two geophones in the analysis presented here.

Results

Calibration relations between geophone parameters and bedload mass

Regarding the minimum particle size for impulse counts, previous measurements at the Erlenbach and in flume experiments have indicated that the geophone signal response becomes much stronger (and thus the number of impulses per unit mass increases) for particle sizes increasing from 20 to 30 mm (Rickenmann *et al.*, 2012). The previous analyses of the calibration measurements at the Erlenbach (with PBIS, Rickenmann and McArdell, 2007; with geophones, Rickenmann *et al.*, 2012) and at the Pitzbach (with PBIS, Rickenmann and McArdell, 2008) showed that *Sum IMP* values (summed impulse counts) increase approximately linearly with bedload mass or volume. Using the calibration data summarized in Table II, it was found that the level of correlation between *Sum IMP* values and bedload mass M for the different field sites did not vary considerably (in terms of the correlation coefficient between values calculated with the regression relation and the *Sum IMP* values) if M is determined for either $D > 10$ mm or D 20 mm. For the remainder of this paper, the higher threshold grain size of $D = 20$ mm has been used to determine total mass, M, but we note that similar results are obtained for a lower threshold grain size of $D = 10$ mm.

We tested calibration relations between the geophone parameters *Sum IMP*, *Sum Max_IP*, *Sum Int_IP*, and *Sum IQA_IP* in turn as the dependent variable and sampled bedload mass as the independent variable (refer to Table III for the definition of the geophone parameters). The resulting calibration relations are illustrated in Figures 3–6, and some statistics of the regression equations are given in Table IV. For the Erlenbach, the Fischbach, and the Ruetz, the most detailed observations are available for the between-site comparison of the calibration measurements (see earlier). For these sites, the statistics of the calibration relations are generally somewhat better than for the other two sites. The following general observations can be made:

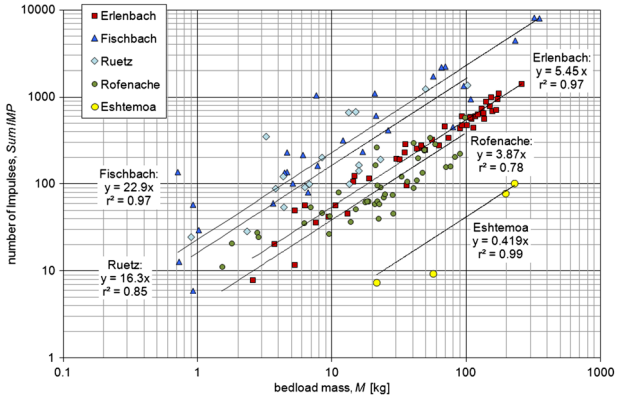

Figure 3. Linear relations of geophone value *Sum IMP* as a function of bedload mass M for the calibration measurements at the different observation sites. This figure is available in colour online at wileyonlinelibrary.com/journal/espl

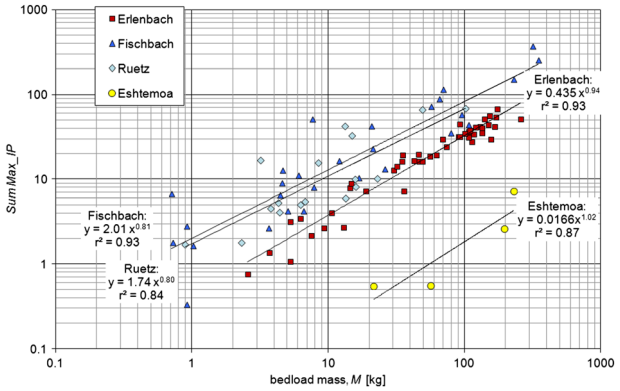

Figure 4. Power law relations of geophone value *Sum Max_IP* as a function of bedload mass M for the calibration measurements at the different observation sites. This figure is available in colour online at wileyonlinelibrary.com/journal/espl

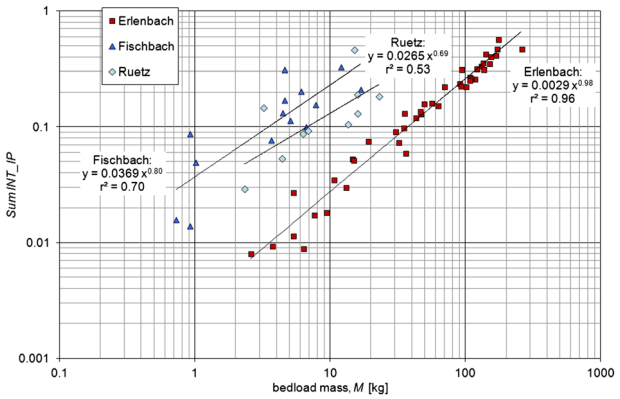

Figure 5. Power law relations of geophone value *Sum INT_IP* as a function of bedload mass M for the calibration measurements at the different observation sites. This figure is available in colour online at wileyonlinelibrary.com/journal/espl

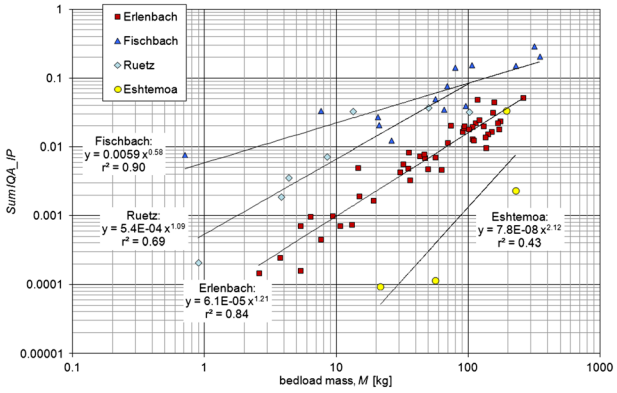

Figure 6. Power law relations of geophone value *Sum IQA_IP* as a function of bedload mass *M* for the calibration measurements at the different observation sites. This figure is available in colour online at wileyonlinelibrary.com/journal/espl

(i) the correlation of the regression models between *Sum IMP* and *M* (linear or power law relations) is generally quite good ($r^2 > 0.85$), and the exponents of a power law relation are relatively close to unity (except for the Rofenache). We determined a simple linear calibration relation with intercept 0 for two reasons: (a) it allows a straightforward comparison of the between-site variation in the strength of the signal response by comparing the linear calibration coefficient k_b; and (b) the correlation coefficients for a linear calibration relation with intercept 0 are larger than for a linear calibration relation with intercept $\neq 0$.

(ii) For each stream, the quality (or goodness of fit) of the regression models (in terms of the correlation coefficient r^2 and the relative standard error s_e; Table IV) relating *Max_IP*, or *Sum Int_IP*, or *Sum IQA_IP* to *M* is similar to that between *Sum IMP* and *M*, except for Ruetz and Eshtemoa with a limited number of data points. However, some of these calibration relations are more non-linear, i.e. the power law exponents deviate more strongly from unity as compared with the *Sum IMP* versus *M* relations.

(iii) The calibration coefficients of the linear calibration relations between those geophone parameters examined and bedload mass *M* differ between sites (see e.g. coefficient k_b in Table IV). The Eshtemoa data plot lower than those of the other channels (Figures 3, 4 and 6) and have the smallest coefficient k_b; this value is less variable among the other sites.

Observations (i) and (ii) indicate that a linear calibration relation between *Sum IMP* and *M* is a good description of the data, and observation (iii) requires explaining through site-specific differences in bed material and transport processes (see later).

Table IV. Coefficients, exponents and statistical properties of the calibration relations obtained from regression between various geophone summary values and bedload mass *M* for the different observation sites.

	Erlenbach	Fischbach	Ruetz	Eshtemoa	Rofenache
Sum IMP = $\mathbf{k_b}$ *M*					
$\mathbf{k_b}$	5.45	22.9	16.3	0.419	3.87
r^2	0.973	0.966	0.853	0.990	0.775
significance level: probability *p*	<0.0001	<0.0001	<0.0001	<0.0009	<0.0001
s_e	0.183	0.449	0.646	0.148	0.484
Sum IMP = $\mathbf{b_1}$ $M^{\mathbf{c1}}$					
b_1	5.30	34.6	28.2	0.143	9.36
c_1	1.01	0.88	0.83	1.18	0.73
r^2	0.973	0.959	0.862	0.994	0.768
significance level: probability *p*	<0.0001	<0.0001	<0.0001	<0.045	<0.0001
s_e	0.188	0.372	0.490	0.110	0.335
Sum Maxima_IP = $\mathbf{b_2}$ $M^{\mathbf{c2}}$					
b_2	0.435	2.01	1.74	0.0166	—
c_2	0.94	0.81	0.80	1.02	—
r^2	0.929	0.926	0.840	0.871	—
significance level: probability *p*	<0.0001	<0.0001	<0.0001	<0.101	
s_e	0.290	0.475	0.522	0.414	
Sum INT_IP = $\mathbf{b_3}$ $M^{\mathbf{c3}}$					
b_3	0.0029	0.0369	0.0265	—	—
c_3	0.98	0.80	0.69	—	—
R^2	0.963	0.698	0.530	—	—
significance level: probability *p*	<0.0001	<0.0001	<0.011		
s_e	0.226	0.489	0.375		
Sum IQA_IP = $\mathbf{b_4}$ $M^{\mathbf{c4}}$					
b_4	6.1 E − 5	0.0059	5.4 E–4	7.8 E–8	—
c_4	1.21	0.58	1.09	2.12	—
r^2	0.839	0.898	0.694	0.427	—
significance level: probability *p*	<0.0001	<0.0001	<0.0021	<0.242	
s_e	0.484	0.267	1.442	0.477	

All calibration relations refer to bedload mass with $D > 20$ mm. In all equations, the units of *M* are in kilograms. Here r^2 is the correlation coefficient between values calculated with the regression relation and the recorded geophone summary values. Similarly, in all figures, r^2 is determined between the predicted *y*-value and the observed *y*-value (in the linear domain). The relative standard error s_e is determined for the values calculated with the regression relation and the recorded geophone summary values, divided by the mean of the recorded geophone summary values.

Effects of grain size and of mean flow velocity on geophone signal

In this section we address how much site-specific conditions affect the geophone signal or the summary values. We first present observations regarding the effects of grain size variations and then consider the effects of different flow conditions.

Effects of grain size variations

For calibration measurements in the Erlenbach, Fischbach, Ruetz, and Rofenache, there is a general coarsening trend of the grain size distribution (GSD) with increasing unit bedload transport rate q_b, as expected from general bedload transport theory (Parker, 2008). This is illustrated using mean GSD determined for different classes of q_b values (Figures 7a and 7b). However, GSDs are quite variable within given classes of q_b and do not necessarily follow the general trend. The coarsening of GSD can also be identified in the geophone summary values for some sites, as is illustrated later. For the Erlenbach, Fischbach and Ruetz, the *b*-axis of the largest transported particle shows a correlation with *MaxMaxA* (maximum amplitude) measured during each calibration period, although the scatter of the data around the power law regression lines is quite large (Figure 8). In addition, the trends of the power law relations are quite similar (Figure 8). However, for this comparison (Figure 8), it should be borne in mind that *MaxMaxA* values for the Fischbach and Ruetz were multiplied by a factor of 1.3 to compensate for the damping of the geophone signal.

We further explored whether other characteristic values of bedload GSD can be related to summary geophone values. For the Erlenbach, Fischbach, and Ruetz, a correlation exists between percentage P_i of grains coarser than a given size D_i (where i is grain size in millimetres), based on a cumulative grain size distribution by mass for all transported bedload particles with $D > 10$ mm. We found that the product *MaxMaxA*Mean*(*MaxA_IP*) is a suitable parameter to be correlated with the P_i values; this parameter includes information on the overall largest particle size via the maximum amplitude (*MaxMaxA*) of the sampling period (Figure 8) and also on the largest particle sizes registered in each one second interval and averaged over the sampling period (*Mean*(*MaxA_IP*)). Different power law regression lines could be identified – for example, between P_{20}, P_{30}, P_{45} and *MaxMaxA*Mean*(*MaxA_IP*), as shown in Figures 9a–9c. These regression lines are best defined in the Erlenbach, followed by the Ruetz and the Fischbach. However, for the Fischbach, the two calibration measurements with the largest q_b values > 1 kg/s m were excluded from Figure 9b; these measurements were associated with the highest discharges and the coarsest bedload samples, they have *MaxMaxA*Mean* (*MaxA_IP*) values about one order of magnitude larger than in Figure 9b and do not match the general power-law trend defined by the rest of the Fischbach data.

Effect of mean flow velocity

To explore how between-site factors may influence the geophone summary values, we determined the linear calibration coefficient of the relation:

$$SumIMP = k_b M \tag{1}$$

While the coefficients k_b as given in Figure 3 and Table IV represent a mean value for all the calibration measurements at a site, we have also determined individual coefficients k_{bj} for each calibration sample using the corresponding $SumIMP_j$

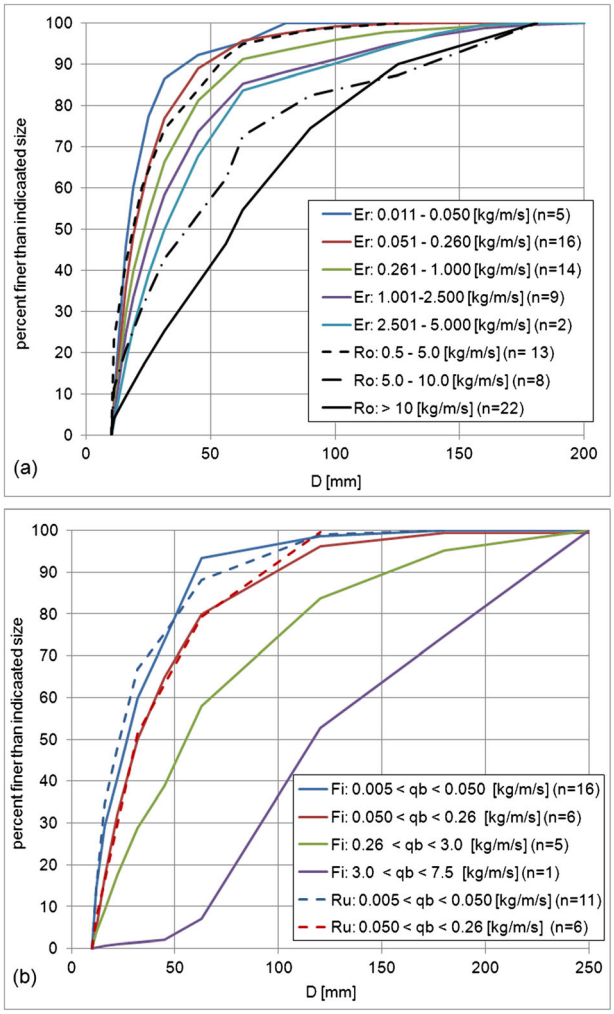

Figure 7. (a) Mean grain size distribution of the bedload material for the Erlenbach (Er) and the Rofenache (Ro), averaged for different classes of unit bedload transport q_b, for $D > 10$ mm. (b) Mean grain size distribution of the bedload material for the Fischbach (Fi) and the Ruetz (Ru), averaged for different classes of unit bedload transport q_b, for $D > 10$ mm.This figure is available in colour online at wileyonlinelibrary.com/journal/espl

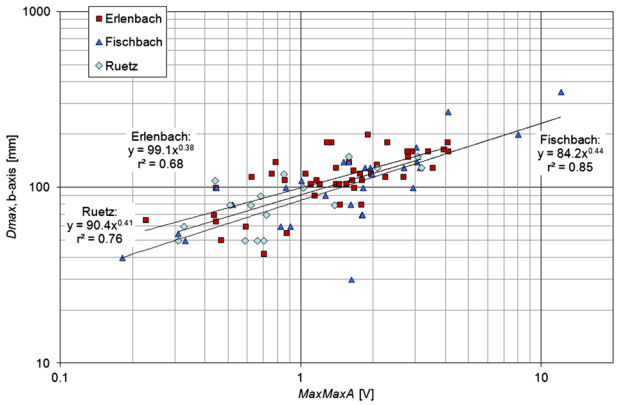

Figure 8. Relation between D_{max} and *MaxMaxA* for the calibration measurements at the different observation sites. The *MaxMaxA* values for the Fischbach and Ruetz were multiplied by a factor of 1.3 to compensate for the damping of the geophone signal.This figure is available in colour online at wileyonlinelibrary.com/journal/espl

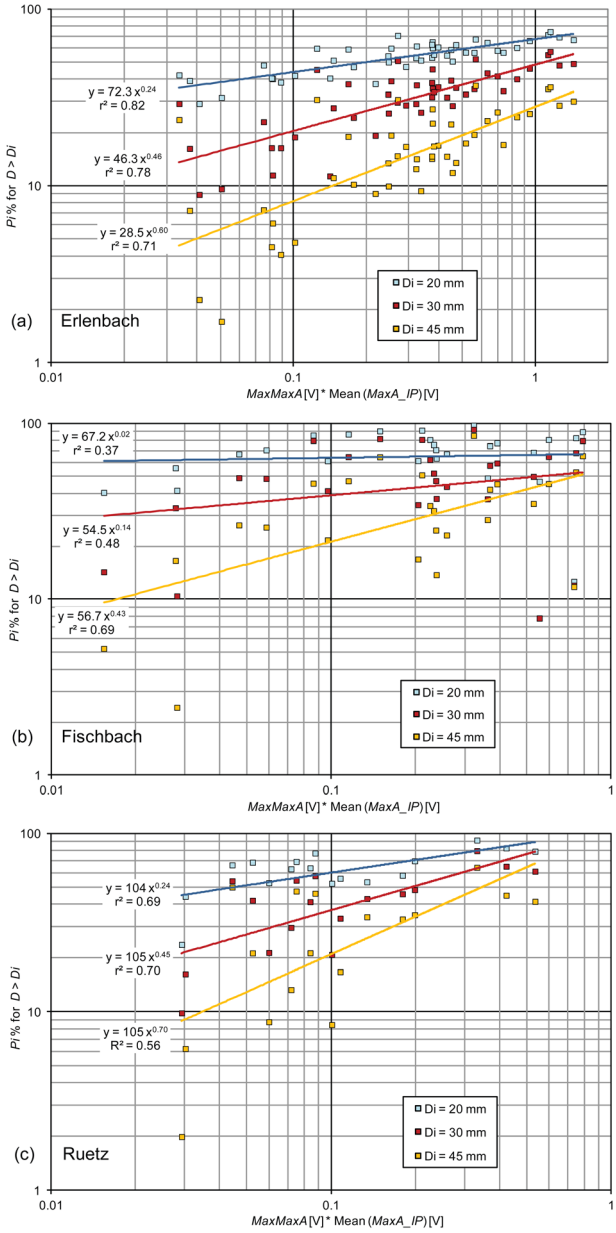

Figure 9. Relations between percentage of grains larger than a limiting grain diameter D_i (for grains with $D > 10$ mm) and *(MaxMaxA) *Mean(MaxA_IP)* for (a) the Erlenbach, (b) the Fischbach (two calibration measurements with the largest q_b values > 1 kg/s m have been excluded), and (c) the Ruetz.This figure is available in colour online at wileyonlinelibrary.com/journal/espl

and M_j values at a given site as (where the subscript j is an index of the sample number):

$$k_{bj} = SumIMP_j / M_j \quad (2)$$

We have plotted the coefficient k_{bj} as a function of the mean flow velocity during the calibration measurements at each site (Figure 10); measurements obtained in flume experiments are included to extend the range of the field data set. The flume experiments include tests with a spherical quartz particle of $D = 40$ mm (Hegglin, 2011) and with natural particles of different sizes and shapes with *b*-axes in size classes $C_1 = 45.3$–63 mm, $C_2 = 63$–80 mm, and $C_3 = 80$–112 mm (Morach, 2011). The measurements indicate that, for mean flow velocities larger than about 2 m/s, both the field and flume measurements tend to show a weaker response of the geophone signal, i.e. on average, a lower number of impulses per unit

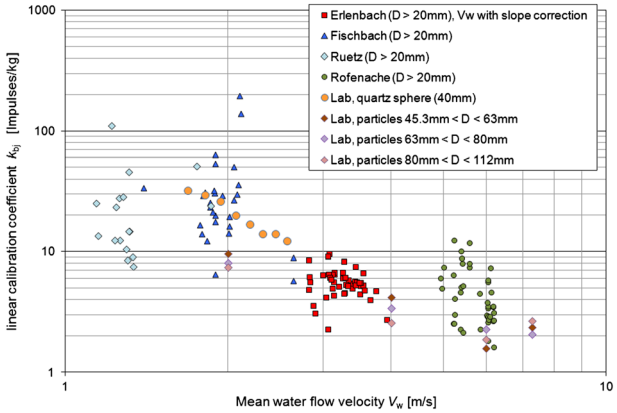

Figure 10. Relation between linear calibration coefficient k_{bj} and mean water velocity V_w for the calibration measurements at the different observation sites. Also included are data from flume experiments with a quartz sphere and with natural particles.This figure is available in colour online at wileyonlinelibrary.com/journal/espl

bedload mass are recorded with increasing mean flow velocity. The data for the flume experiments with natural particles plot in the lower part of the range of the field data. They show a smaller coefficient k_{bj} with increasing grain sizes for flow velocities of 2 m/s and 4 m/s, while this trend is not confirmed for higher flow velocities of 6 m/s and 7.3 m/s (Figure 10). If the range of tested grain sizes in the flume (40 mm < D < 112 mm) is compared with the GSD in Figures 7a and 7b, it is evident that the large majority of field data also includes a substantial proportion of finer particles than those used for the flume experiments.

Discussion

General behaviour of the geophone measuring system

In this section, we discuss first those characteristics of the Swiss plate geophone measuring system, which are similar at the field sites investigated. We then address the importance of accounting for signal noise particularly when using the geophone summary value *Sum INT*. Finally, we summarize our interpretation of the similarity of geophone summary values at the sites.

In the analysis earlier we have presented the calibration relations in terms of geophone summary values (such as *Sum IMP*) versus bedload mass and not in terms of impulse rates versus bedload transport rate because we found, in an earlier study, that increasing the integration time reduces the scatter of the calibration data, by averaging stochastic factors such as impact location on a given plate, type of particle motion and impact velocity (Rickenmann and McArdell, 2007, 2008). If the analysis were made in terms of rates, the general findings would not change.

For the majority of the sites investigated, we do not have records of the raw signals. To examine whether the shape of the signal may be similar between sites, we compared, therefore, the geophone summary values. The shape of a typical geophone signal (Figure 2) makes it evident that the various summary values such as *Sum IMP, Sum Max_IP, Sum IQA_IP, Sum INT_IP-noN* (see Table III) that are derived from the same raw signal are necessarily related and correlate strongly (Figures 11a–11c). A rather strong correlation exists between *Sum Max_IP* and *Sum IMP* (Figure 11a), *Sum IQA_IP* and *Sum IMP* (Figure 11b) and there is a somewhat less strong correlation between *Sum INT_IP- noN* and *Sum IMP* (Figure 11c).

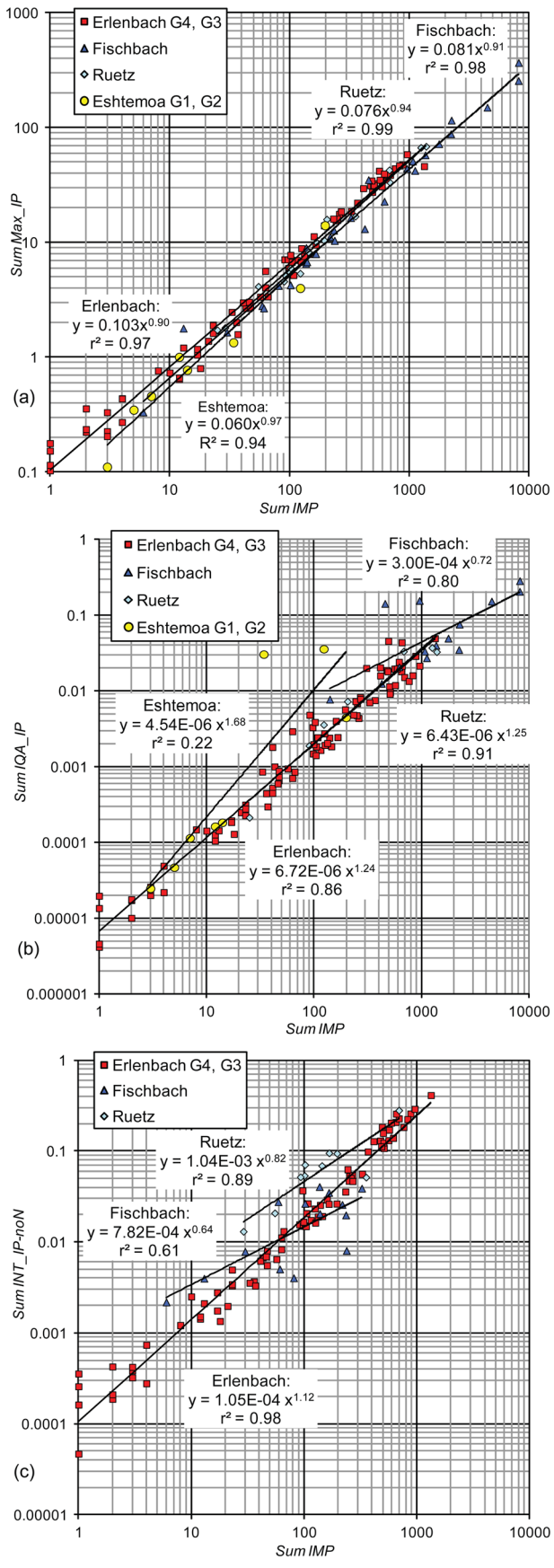

Figure 11. Relation between different geophone summary values for the calibration measurements at the different observation sites: (a) *Sum Max_IP* versus *Sum IMP*, (b) *Sum IQA_IP* versus *Sum IMP*, (c) *Sum INT_IP-noN* versus *Sum IMP*.This figure is available in colour online at wileyonlinelibrary.com/journal/espl

Effect of signal noise on summary values

The "noise" of the geophone system during periods without bedload transport (e.g. at very low discharges) is typically around a few millivolts, i.e. the geophone signal randomly fluctuates around 0 V by a few millivolts. The selected threshold value A_{min} for the impulse count was empirically determined and it guarantees that increased turbulence of flow at higher discharges does not add to the impulse counts. With regard to the *Sum Max_IP* values, noise is irrelevant because only the largest amplitude value is recorded each second during the calibration measurements. Summing only the values of those one second intervals for which at least one impulse was observed (*Time_IP* values) eliminates the noise for the periods with no bedload transport or with only very weak bedload transport (i.e. when no impulse is recorded).

From the raw signals recorded at the Erlenbach during the calibration measurements, we know that the bedload particle impacts cause the geophone signal to exceed the threshold value A_{min} during only a small fraction of time, hence the *Sum INT_IP* values include a substantial portion of noise. Therefore, a mean noise value was determined over the calibration periods (one second values) when no impulses were recorded: this mean noise amplitude level (*NAL*) is 0.89 mV (sensor G3) and 1.0 mV (sensor G4) in the Erlenbach, 3.0 mV (sensor G4) in the Fischbach, and 1.1 mV (sensor G4) in the Ruetz. The product of *NAL*Time_IP* was subtracted from the *Sum INT_IP* values to derive the *Sum INT_IP-noN* values. As observed in Figure 11c, the *Sum INT_IP-noN* versus *Sum IMP* values plot around a similar mean relation for the data of all the different sites. If *Sum INT_IP* versus *Sum IMP* values are plotted (not shown here), then the *Sum INT_IP* values from the Fischbach and Ruetz are twice as large as those of the Erlenbach. With the *Sum IQA_IP* values, less noise is included because the smaller amplitudes contribute with much less weight to the summary value than the larger amplitudes. If a similar correction for noise (reduction of *IQA* values) is made as for the *Sum INT_IP* values, this correction is typically less than 10% of the *Sum IQA_IP* values. The Fischbach data in the plot *Sum IQA_IP* versus *Sum IMP* values (Figure 11b) show a somewhat larger scatter and a deviation from the general trend as compared with the data for the Erlenbach and the Ruetz. It is unclear what causes this deviation, but it may be associated with the fact that these particular data of the Fischbach pertain to flows with the highest bedload fluxes and, hence, generally coarser particles (see Table II and Figure 7). The earlier analysis suggests that, particularly in the determination of the *Sum INT* summary values, it is important to account for noise in the signal.

Implication of similarity between summary values

The analysis shown in Figures 11a–11c suggests that the relations involving the geophone summary values are essentially site-independent (at least for calibration events with *Sum IMP* values up to about 2000 impulses, see Figure 11c) and that these relations are likely to reflect internal characteristics of the measuring system. This implies that the shape of the signal response is similar at the sites investigated. In this context, it is also interesting to note that the relations of maximum particle size to signal amplitude are similar amongst the study sites (Figure 8) and independent of local conditions. The similarity between the various summary values also suggests that the simple parameter *Sum IMP* is as suitable as any of the other parameters in serving as an indicator of transported bedload mass.

Effects of flow and particle conditions on geophone signal response

In this section, we summarize our interpretation of the factors which are likely to be responsible for between-site differences in signal response. We first discuss how different particles sizes affect the impulse counts. These observations are based on flume experiments because, at the field sites, it is not possible to identify the signal caused by single particles of the mixed sizes making up the bedload. We then address the influence of mean flow velocity and particle motion on the geophone signal response. Finally, we give an outlook for further investigations.

Effect of particle size on geophone signal

For coarse to medium gravel and finer particles, the signal response is expected to decrease with decreasing particle size near the detection threshold for small particles. This was observed in flume tests using sedimentary particles from the Erlenbach, where the number of impulses per unit mass strongly increases for particles with mean weights increasing from 25 to 50 to 75 g, corresponding with mean *b*-axes of 26, 31, and 37 mm (Böckli, 2011). However, flume experiments using the PBIS and very coarse gravel to cobbles from the Erlenbach showed that the number of impulses per unit mass decreased approximately linearly with grain size D, for mean particle sizes (*b*-axis) in the range 40–200 mm (Etter, 1996). Thus, there is an overall trend for the k_{bj} values to first increase and then to decrease with increasing particle size or mass. This trend is confirmed by flume experiments with the Swiss geophone plate using spherical quartz particles with diameters of 10, 20 mm (50 runs for each size), 30, 33, 40, 59, and 76 mm (100 runs for each size) and a mean water velocity of 1.9 m/s (Hegglin, 2011). These experiments show maximal signal response (in terms of impulses per unit mass) for a sphere weight of 89 g, corresponding to a diameter of 40 mm (Figure 12). Our interpretation of this behaviour is that there is an optimum particle size (or mass) which produces most impulses per unit mass. If particles are smaller, some of them will not have enough momentum to produce any impulses. If particles are larger, the increased momentum may result in larger amplitudes of the signal and, probably, further impulses during the attenuation of the signal; however, this effect appears to be overcompensated by the reduced number of particles per unit mass, resulting in less impact events. A similar observation was made by Møen *et al.* (2010) in flume experiments using an accelerometer fixed to a 10 mm thick steel plate on the bed: maximal acoustic signal response was detected for an intermediate grain size class of 1 to 2 mm, over a range of particle sizes investigated from 0.25 to 16 mm. Thus, for the geophone calibration relations with *Sum IMP*, the impulse count is related to the bedload mass by a mean coefficient (k_b coefficient in Equation 1), which represents variable relative contributions from particles of different sizes and includes further variations due to stochastic factors such as type of particle motion, impact velocity, and impact location on the steel plate (cf. Turowski *et al.*, 2013).

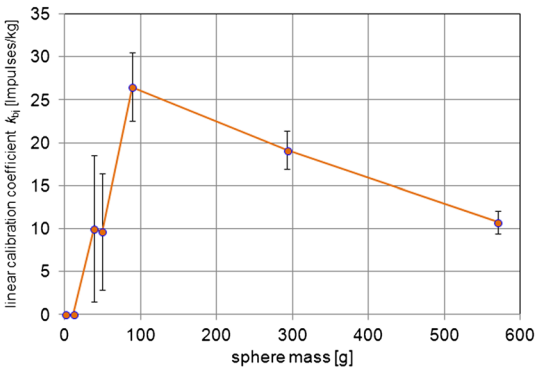

Figure 12. Linear calibration coefficient k_{bj} versus particle weight of quartz spheres of different sizes, based on flume experiments with the Swiss plate geophone and a water flow velocity of 1.9 m/s. The data points show the mean and standard deviation of 100 repeated runs (for D larger than 30 mm or for masses larger than 38 g). The maximum k_b value corresponds to a sphere diameter of 40 mm. This figure is available in colour online at wileyonlinelibrary.com/journal/espl

Effect of mean flow velocity and particle motion on geophone signal

The data of the geophone calibration measurements, both from the field sites and flume experiments, indicate a decreasing strength of the geophone signal for increasing mean water flow velocities greater than about 2 m/s, i.e. the number of impulses per unit bedload mass (k_b coefficient in Equation 1 and k_{bj} coefficient in Equation 2) tends to decrease with increasing mean flow velocity (Figure 10). Earlier investigations using PBISs had also shown a substantial difference in the k_b values between the Pitzbach mountain stream and the Erlenbach and it was speculated that part of this difference might be due to different water velocities (Rickenmann and McArdell, 2008). One could argue that an increase in flow and hence particle velocities would increase the impact energy of a particle on the plate and that this would cause the plate to vibrate longer after impact, thereby causing more impulses from one impact. Such an effect may indeed be important when increasing particle sizes or weights (and hence impact energy) produce larger signal amplitudes (as shown in Figure 8). However, if increasing particle velocities result in flatter (more bed-parallel) trajectories, then it is likely that the increase in particle momentum may be less relevant for the impact energy and that the number of impact events may decrease, as is suggested by empirical evidence (Figure 10). The number of impacts is expected to be affected by local conditions such as particle velocity, particle shape, number of particles per unit bedload mass, and saltation lengths. In fact, several flume studies have demonstrated that saltation height and saltation length of bedload particles depend on shear or excess shear stress (Lajeunesse *et al.*, 2010) and thus on flow velocity. Flume experiments both with the Swiss geophone plate (Turowski and Rickenmann, 2009) and using a hydrophone fixed to a steel plate at the bed (Krein *et al.*, 2008) confirm the influence of particle motion (sliding, rolling) on the signal response. In principle, one may also expect that changing bed morphology upstream of the geophone plates may affect the transport mode, and contribute to some scatter in the calibration relation if direct measurements were taken at different times. This aspect is likely to be less important at the Erlenbach and the Rofenache sites, which have an artificial proximal flow channel.

Outlook for further investigations

In summary, these studies of the Swiss plate geophone system indicate that, for natural bedload particles and for a given site, a unique calibration relation between a mean k_{bj} value and grain size D exists for a given mean flow (or particle) velocity, similar to that which is illustrated in Figure 12 for a quartz sphere. For a given grain size and flow velocity, the signal response (i.e. the k_b or k_{bj} value) is expected to vary according to location of impact on the plate, grain shape, and type of movement (sliding, rolling, saltating), as was observed in flume

experiments using either a PBIS (Etter, 1996) and a geophone sensor (Turowski and Rickenmann, 2009; Böckli, 2011; Hegglin, 2011). By performing systematic flume experiments with natural bedload particles from a given site within the range of flow velocities to be expected in the field, the calibration relation k_{bj} = function of (D, V_w) can be determined using a representative mixture of grain shapes for a given size class, and also the uncertainty of the estimated k_{bj} values can be determined by repeating the experiments with identical conditions. Similar systematic flume experiments may also help to constrain the GSD of the transported material, as is suggested by the data shown in Figure 9. Further investigations to understand better the geophone signal response are under way. They offer the perspective that the derivation of a flume-based functional relation between the linear coefficient k_{bj} and particle size D, combined with an estimate of the GSD based on the geophone signal, may allow the development of a calibration relation without the need for calibration measurements in the field.

Weak geophone signal response in the Eshtemoa

The calibration data for the Nahal Eshtemoa show a much weaker signal response than for the other streams (Figures 3, 4, and 6) for a given bedload mass. If the grain size distribution from the LC sampler is truncated at 10 mm, the D_{50} is 12 mm and the D_{84} is 35 mm, which is generally much finer-grained by comparison with the samples from the calibration measurements for the other study streams (Figure 7). Given a critical particle size of about 20 to 30 mm for detection of geophone impulses (Figure 12; Böckli, 2011; Rickenmann *et al.*, 2012), the finer bedload grain sizes of the Nahal Eshtemoa calibration data may explain in part the weak signal response. In addition, as much of the bedload at the Eshtemoa comprises granules and small pebbles and as the approach reach to the Eshtemoa samplers is often cross-sectionally sub-horizontal, some of the mobile bed particles are transported as thin gravel sheets (in the sense of Whiting *et al.*, 1988) at high bedload fluxes. This may result in temporary deposition of gravel particles over part of the geophone plates, inducing a cover or protection effect, thus reducing the signal response (Turowski and Rickenmann, 2009).

Conclusions

Indirect bedload transport measurements have been made with the Swiss plate geophone system in five gravel-bed mountain streams. For the calibration of the geophone system, direct bedload samples were obtained while signals were being recorded – between 17 and 46 pairs of records per site, except in the Eshtemoa, where infrequent bedload events have, so far, yielded only four data pairs. Geophone summary values have been derived to represent mean characteristics of the raw signal over one second intervals. The principal geophone summary values (summed Impulses, summed Maximum Amplitudes, Integrals, and Quadratic Integrals) show a good to reasonable correlation with the transported bedload mass. These summary values are generally strongly inter-correlated for a given measuring site and the functional relations obtained are similar between the sites. These functional relations are likely to reflect internal characteristics of the measuring system, implying that the shape of the geophone signal response is similar at the sites investigated.

The number of impulses, i.e. the number of peaks above a pre-defined threshold value of the geophone output signal, was found to be a robust summary parameter. The calibration measurements at all sites show an approximately linear relation between number of impulses and bedload mass transported over the sensors. By comparing the calibration measurements from the different field sites and given insights obtained during preliminary flume experiments, the main factors influencing the geophone signal response have been identified. The mean number of impulses per unit bedload mass appears to depend on the mean flow velocity V_w during the calibration measurement, for the range $2\ \text{m/s} < V_w < 7\ \text{m/s}$. Larger flow velocities are likely associated with larger particle velocities, possibly increasing both saltation lengths of particles and a preference for sliding over rolling motion, both of which could explain a weaker signal response with increasing flow velocities. In addition, the flume experiments suggest that the number of impulses for a given bedload mass is a function of particle size, reaching a maximum at $D \approx 40$ mm for spherical quartz particles.

For the Erlenbach, Fischbach and Ruetz, the *b*-axis of the largest transported particle shows a correlation with the maximum amplitude (*MaxMaxA*) measured during each calibration period, although the scatter of the data around the power law regression lines is quite large. In addition, the mean trends of the power law relations are quite similar. For these three sites, a correlation exists between percentage P_i of grains coarser than a given size D_i and the product *MaxMaxA*Mean* (*MaxA_IP*). The corresponding regression lines are best defined for the Erlenbach, followed by the Ruetz and the Fischbach, indicating that the geophone signal also contains some information on the bedload grain size. Flume and field experiments should further allow exploration of the possibility of extracting information, among others, about the grain size of the particles responsible for the geophone signal response.

Acknowledgements—The authors are grateful to the Tyrolean Water Power Company (TIWAG) for performing the geophone calibration measurements in the Fischbach and Ruetz streams and for providing these data to WSL for further analysis. The authors acknowledge the support of the Tyrolean Hydrographic Service for supporting the Rofenache measurements. The study was supported by SNF grant 200021_124634/1 to DR, SNF grant 200021_137681/1 to DR and JMT, and ISF grant 1073–09 to JL. The authors thank the members of the mountain hydrology research unit at WSL for help in the field. They also thank the reviewers and the Associate Editor for their comments which helped improving the manuscript.

References

Alexandrov Y, Laronne JB, Reid I. 2007. Intra-event and inter-seasonal behaviour of suspended sediment in flash floods of the semi-arid northern Negev, Israel. *Geomorphology* **85**: 85–97. DOI: 10.1016/j.geomorph.2006.03.013

Alexandrov Y, Balaban N, Bergman N, Chocron M, Laronne JB, Powell DM, Reid I, Tagger S, Wener-Frank I. 2009. Differentiated suspended sediment transport in headwater basins of the Besor catchment, northern Negev. Israel. *Journal of Earth Science* **57**: 177–188. DOI: 10.1560/IJES.57.3-4.177

Bänziger R, Burch H. 1990. Acoustic sensors as indicators for bed load transport in a mountain torrent. In *Hydrology in Mountainous Regions I*, Lang H, Musy A (eds), IAHS Publication no. 193. IAHS: Wallingford; 207–214.

Barton JS, Slingerland RL, Pittman S, Gabrielson TB. 2010. Monitoring coarse bedload transport with passive acoustic instrumentation: a field study. In *Bedload-surrogate Monitoring Technologies*, Gray JR, Laronne JB, Marr JDG (eds), US Geological Survey Scientific Investigations Report 2010–5091. US Geological Survey: Reston, VA; 38–51. http://pubs.usgs.gov/sir/2010/5091/papers/listofpapers.html

Bassett C, Thomson J, Polagye B. 2013. Sediment-generated noise and bed stress in a tidal channel. *Journal Geophysical Research – Oceans* **118**: 2249–2265. DOI: 10.1002/jgrc.20169

Belleudy P, Valette A, Graff B. 2010. Passive hydrophone monitoring of bedload in river beds: first trials of signal spectral analyses. In *Bedload-surrogate Monitoring Technologies*, Gray JR, Laronne JB, Marr JDG (eds), US Geological Survey Scientific Investigations Report 2010–5091. US Geological Survey: Reston, VA; 67–84. http://pubs.usgs.gov/sir/2010/5091/papers/listofpapers.html

Bergman N, Laronne JB, Reid I. 2007. Benefits of design modifications to the Birkbeck bedload sampler illustrated by flash-floods in an ephemeral gravel-bed channel. *Earth Surface Processes and Landforms* **32**: 317–328. DOI: 10.1002/esp.1453

Böckli M. 2011. Laborversuche zum Verhalten von Geophon-Sensoren, Master Thesis. ETH Zürich and WSL Birmensdorf; 56 pp.

Bogen J, Møen K. 2003. Bed load measurements with a new passive acoustic sensor. In *Erosion and Sediment Transport Measurement in Rivers: Technological and Methodological Advances*, Bogen J, Fergus T, Walling DE (eds), IAHS Publication no. 283. IAHS: Wallingford; 181–192.

Bunte K, Abt SR. 2003. Sampler size and sampling time affected bed load transport rates and particle size measured with bed load traps in gravel-bed streams. In *Erosion and Sediment Transport Measurement in Rivers: Technological and Methodological Advances*, Bogen J, Fergus T, Walling DE (eds), IAHS Publication no. 283. IAHS: Wallingford; 126–133.

Camenen B, Jaballah M, Geay T, Belleudy P, Laronne JB, Laskowski JP. 2012. Tentative measurements of bedload transport in an energetic alpine gravel bed river. In *River Flow 2012*, Muñoz RM (ed.). CRC Press: Boca Raton, FL.

Cohen H, Laronne JB, Reid I. 2010. Simplicity and complexity of bedload response during flash floods in a gravel-bed ephemeral river: a 10-year field study. *Water Resources Research* **46**: W11542. DOI: 10.1029/2010WR009160

Downing J. 2010. Acoustic gravel-momemtum sensor. In *Bedload Surrogate Monitoring Technologies*, Gray JR, Laronne JB, Marr JDG (eds), US Geological Survey Scientific Investigations Report 2010–5091. US Geological Survey: Reston, VA; 143–158. http://pubs.usgs.gov/sir/2010/5091/papers/listofpapers.html

Downing J, Farley PJ, Bunte K, Swingle K, Ryan SE, Dixon M. 2003. Acoustic gravel-transport sensor: description and field tests in Little Granite Creek, Wyoming, USA. In *Erosion and Sediment Transport Measurement in Rivers: Technological and Methodological Advances*, Bogen J, Fergus T, Walling DE (eds), IAHS Publication no. 283. IAHS: Wallingford; 193–200.

Etter M. 1996. Zur Erfassung des Geschiebetransportes mit Hydrophonen, Diploma Thesis. University of Berne and WSL Birmensdorf; 110 pp.

Ferguson R. 2007. Flow resistance equations for gravel and boulder bed streams. *Water Resources Research* **43**: W05427. DOI: 10.1029/2006WR005422

Froehlich W. 2003. Monitoring bed load transport using acoustic and magnetic devices. In *Erosion and Sediment Transport Measurement in Rivers: Technological and Methodological Advances*, Bogen J, Fergus T, Walling DE (eds), IAHS Publication no. 283. IAHS: Wallingford; 201–210.

Froehlich W. 2010. Monitoring of bed load transport within a small drainage basin in the Polish flysch Carpathians. In *Bedload-surrogate Monitoring Technologies*, Gray JR, Laronne JB, Marr JDG (eds), US Geological Survey Scientific Investigations Report 2010–5091. US Geological Survey: Reston, VA; 185–194. http://pubs.usgs.gov/sir/2010/5091/papers/listofpapers.html

Geay T. 2013. Mesure acoustique passive du transport par charriage dans les rivières. [Passive acoustic measurement of bedload transport in rivers] PhD Thesis, Université Joseph Fourier, Grenoble, France. [in French].

Gray JR, Laronne JB, Marr JDG (eds). 2010. Bedload-surrogate Monitoring Technologies, US Geological Survey Scientific Investigations Report 2010–5091. US Geological Survey: Reston, VA. http://pubs.usgs.gov/sir/2010/5091/

Habersack H, Seitz H, Liedermann M. 2010. Integrated automatic bedload transport monitoring. In *Bedload-surrogate Monitoring Technologies*, Gray JR, Laronne JB, Marr JDG (eds), US Geological Survey Scientific Investigations Report 2010–5091. US Geological Survey: Reston, VA; 218–235. http://pubs.usgs.gov/sir/2010/5091/papers/listofpapers.html

Hegg C, McArdell BW, Badoux A. 2006. One hundred years of mountain hydrology in Switzerland by the WSL. *Hydrological Processes* **20**: 371–376.

Hegglin R. 2011. Beiträge zum Prozessverständnis des fluvialen Geschiebetransports, Diploma Thesis. University of Berne and WSL Birmensdorf; 87 pp.

Krein A, Klinck H, Eiden M, Symader W, Bierl R, Hoffmann L, Pfister L. 2008. Investigating the transport dynamics and the properties of bedload material with a hydro-acoustic measuring system. *Earth Surface Processes and Landforms* **33**: 152–163. DOI: 10.1002/esp.1576

Lajeunesse E, Malverti L, Charru F. 2010. Bed load transport in turbulent flow at the grain scale: experiments and modeling. *Journal of Geophysical Research* **115**: F04001. DOI: 10.1029/2009JF001628

Mader H, Seidl T, Wimmer R. 1996. *Abflußregime österreichischer Fließgewässer. Beitrag zu einer bundesweiten Fliessgewässertypologie*. Federal Environment Agency: Vienna; 120 pp.

Mizuyama T, Oda A, Laronne JB, Nonaka M, Matsuoka M. 2010a. Laboratory tests of a Japanese pipe geophone for continuous acoustic monitoring of coarse bedload. In *Bedload-surrogate Monitoring Technologies*, Gray JR, Laronne JB, Marr JDG (eds), US Geological Survey Scientific Investigations Report 2010–5091. US Geological Survey: Reston, VA; 319–335. http://pubs.usgs.gov/sir/2010/5091/papers/listofpapers.html

Mizuyama T, Laronne JB, Nonaka M, Sawada T, Satofuka Y, Matsuoka M, Yamashita S, Sako Y, Tamaki S, Watari M, Yamaguchi S, Tsuruta K. 2010b. Calibration of a passive acoustic bedload monitoring system in Japanese mountain rivers. In *Bedload-surrogate Monitoring Technologies*, Gray JR, Laronne JB, Marr JDG (eds), US Geological Survey Scientific Investigations Report 2010–5091. US Geological Survey: Reston, VA; 296–318. http://pubs.usgs.gov/sir/2010/5091/papers/listofpapers.html

Møen KM, Bogen J, Zuta JF, Ade PK, Esbensen K. 2010. Bedload measurement in rivers using passive acoustic sensors. In *Bedload-surrogate Monitoring Technologies*, Gray JR, Laronne JB, Marr JDG (eds), US Geological Survey Scientific Investigations Report 2010–5091. US Geological Survey: Reston, VA; 336–351. http://pubs.usgs.gov/sir/2010/5091/papers/listofpapers.html

Morach, S. 2011. Geschiebemessungen mittels Geophonen bei hohen Fliessgeschwindigkeiten – Hydraulische Modellversuche, Master Thesis. ETH Zürich and WSL Birmensdorf; 42 pp.

Müller G, Godina R, Gattermayr W. 2009. Der Pegel Vent/Rofenache – Herausforderungen für eine hydrographische Messstelle in einem vergletscherten Einzugsgebiet. *Bulletin of the Hydrographic Service in Austria* **86**: 131–134.

Papanicolaou AN, Knapp D. 2010. A particle tracking technique for bedload motion. In *Bedload-surrogate Monitoring Technologies*, Gray JR, Laronne JB, Marr JDG (eds), US Geological Survey Scientific Investigations Report 2010–5091. US Geological Survey: Reston, VA; 352–366. http://pubs.usgs.gov/sir/2010/5091/papers/listofpapers.html

Parker G. 2008. Transport of gravel and sediment mixtures. In *ASCE Manual 54 – Sedimentation Engineering: Processes, Measurements, Modeling, and Practice*, Garcia MH (ed.). American Society of Civil Engineers (ASCE): Reston, VA; 165–251.

Powell DM, Reid I, Laronne JB, Frostick LE. 1998. Cross stream variability of bedload flux in narrow and wider ephemeral channels during desert flash floods. In *Gravel-bed Rivers in the Environment*, Klingeman P, Beschta R, Komar P, Bradley B (eds). Water Resources Publications, LLC: Highlands Ranch, CO; 177–196.

Powell DM, Reid I, Laronne JB. 1999. Hydraulic interpretation of cross-stream variations in bed-load transport. *Journal of Hydraulic Engineering* **125**: 1243–1252.

Powell DM, Reid I, Laronne JB. 2001. Evolution of bedload grain-size distribution with increasing flow strength and the effect of flow duration on the calibre of bedload sediment yield in ephemeral gravel-bed rivers. *Water Resources Research* **37**: 1463–1474.

Powell DM, Laronne JB, Reid I, Barzilai R. 2012. The bed morphology of upland single-thread channels in semi-arid environments: evidence of repeating bedforms and their wider implications for gravel-bed rivers. *Earth Surface Processes and Landforms* **37**: 741–753. DOI: 10.1002/esp.3199

Raven EK, Lane SN, Ferguson R. 2010. Using sediment impact sensors to improve the morphological sediment budget approach for estimating bedload transport rates. *Geomorphology* **119**: 125–134.

Reid I, Laronne JB, Powell DM. 1998. Flashflood and bedload dynamics of desert gravel-bed streams. *Hydrological Processes* **12**: 543–557.

Reid SC, Lane SN, Berney JM. 2007. The timing and magnitude of coarse sediment transport events within an upland gravel-bed river. *Geomorphology* **83**: 152–182.

Richardson K, Benson I, Carling PA. 2003. An instrument to record sediment movement in bedrock channels. In *Erosion and Sediment Transport Measurement in Rivers: Technological and Methodological Advances*, Bogen J, Fergus T, Walling DE (eds), IAHS Publication no. 283. IAHS: Wallingford; 228–235.

Rickenmann D. 1997. Sediment transport in Swiss torrents. *Earth Surface Processes and Landforms* **22**: 937–951.

Rickenmann D, Fritschi B. 2010. Bedload transport measurements using piezoelectric impact sensors and geophones. In *Bedload-surrogate Monitoring Technologies*, Gray JR, Laronne JB, Marr JDG (eds), US Geological Survey Scientific Investigations Report 2010–5091. US Geological Survey: Reston, VA; 407–423. http://pubs.usgs.gov/sir/2010/5091/papers/listofpapers.html

Rickenmann D, McArdell BW. 2007. Continuous measurement of sediment transport in the Erlenbach stream using piezoelectric bedload impact sensors. *Earth Surface Processes and Landforms* **32**: 1362–1378.

Rickenmann D, McArdell BW. 2008. Calibration of piezoelectric bedload impact sensors in the Pitzbach mountain stream. *Geodinamica Acta* **21**: 35–52.

Rickenmann D, Recking A. 2011. Evaluation of flow resistance in gravel-bed rivers through a large field dataset. *Water Resources Research* **7**: W07538. DOI: 10.1029/2010WR009793

Rickenmann D, Turowski JM, Fritschi B, Klaiber A, Ludwig A. 2012. Improved sediment transport measurements in the Erlenbach stream including a moving basket system. *Earth Surface Processes and Landforms* **37**: 1000–1011. DOI: 10.1002/esp.3225

Taniguchi S, Itakura Y, Miyamoto K, Kurihara J. 1992. A new acoustic sensor for sediment discharge measurement. In *Erosion and Sediment Transport Monitoring Programmes in River Basins*, Bogen J, Walling DE, Day TJ (eds), IAHS publication no. 210. IAHS: Wallingford; 135–142.

Thorne PD. 1986a. Laboratory and marine measurements on the acoustic detection of sediment transport. *Journal of the Acoustic Society of America* **80**: 899–910.

Thorne PD. 1986b. An intercomparison between visual and acoustic detection of seabed gravel movement. *Marine Geology* **72**: 11–31.

Thorne PD, Hanes DM. 2002. A review of acoustic measurements of small-scale sediment processes. *Continental Shelf Research* **22**: 603–632.

Turowski JM, Rickenmann D. 2009. Tools and cover effects in bedload transport observations in the Pitzbach, Austria. *Earth Surface Processes and Landforms* **34**: 26–37. DOI: 10.1002/esp.1686

Turowski JM, Rickenmann D. 2011. Measuring the statistics of bedload transport using indirect sensors. *Journal of Hydraulic Engineering* **137**: 116–121. DOI: 10.1061/(ASCE)HY.1943-7900.0000277

Turowski JM, Yager EM, Badoux A, Rickenmann D, Molnar P. 2009. The impact of exceptional events on erosion, bedload transport and channel stability in a step-pool channel. *Earth Surface Processes and Landforms* **34**: 1661–1673. DOI: 10.1002/esp.1855

Turowski JM, Badoux A, Rickenmann D. 2011. Start and end of bedload transport in gravel bed rivers. *Geophysical Research Letters* **38**: L04401. DOI: 10.1029/2010GL046558

Turowski JM, Böckli M, Rickenmann D, Beer AR. 2013. Field measurements of the energy delivered to the channel bed by moving bedload and links to bedrock erosion. *Journal of Geophysical Research - Earth Surface*. DOI: 10.1002/2013JF002765

Whiting PJ, Dietrich WE, Leopold LB, Drake TG, Shreve RL. 1988. Bedload sheets in heterogeneous sediment. *Geology* **16**: 105–108.